Graphical user interface and experiment control software at the MX beamlines at EMBL Hamburg

Ivars Karpics, Gleb Bourenkov, Marina Nikolova, Thomas R. Schneider

European Molecular Biology Laboratory (EMBL) Hamburg Unit c/o DESY, Notkestrasse 85, 22607, Hamburg, Germany

E-mail: `karpics@embl-hamburg.de`

Abstract. The EMBL Hamburg outstation, located on the DESY Campus (Hamburg Germany), operates two macromolecular crystallography beamlines P13 and P14 on the PETRAIII storage ring. Both beamlines are equipped with high-end instrumentation such as adaptive X-ray optics, configurable compound refractive lenses, beam conditioning units, kappa goniostats, PILATUS detectors, and automatic sample changers to fulfil the needs of the MX community. For the high-level control of the beamlines and data acquisition the MxCuBE (Gabadinho *et al.*, 2010) interface is used. The growing complexity of experiments requires easy and fast adaptation of the control software. The data model and overall architecture of MxCuBE allows implementing new data collection methods and strategies (large scale grid scans, serial crystallography experiments, etc.). EMBL Hamburg is part of the MxCuBE collaboration (http://mxcube.github.io/mxcube/) and actively participates in the software co-development. The overall infrastructure of graphical user interfaces (as running on the Qt4 library), experiment control, on-line data processing and the ISPyB experiment information system at EMBL Hamburg MX beamlines will be presented.

1. Introduction

The macromolecular crystallography (MX) beamlines P13 and P14 at EMBL Hamburg are in user operation since late 2012. With a minimum focus size of 30 x 20 μm^2 (divergence <0.15 μrad) and X-ray energy tunability between 4.0 and 17.5 keV P13 is well suited for crystallographic phasing experiments (Cianci *et al.*, 2015; Cianci *et al.*, 2016). Using an adaptive focusing system the beam can be defocused to a size of 140 x 70 μm. Additionally apertures are used to adjust the beam size. Crystals are positioned and rotated in the X-ray beam with an MD2 diffractometer (Cipriani *et al.* 2007) equipped with a mini-kappa goniostat. The micro-focus beamline P14 is capable of offering a 5 x 5 μm beam with a divergence below 0.3 μrad. In addition to the micro-focused beam a collimated, homogeneous, and quasi-parallel beam with a maximum size of 300 μm can be produced by using Compound Refractive Lenses (CRLs) as mounted in a transfocator (Vaughan *et al.*, 2011). Toggling between micro-focused and collimated conditions takes less than 20 seconds in either direction. P14 is tunable between 6 and 20 keV. For crystal handling an MD3 diffractometer with a vertical spindle axis is installed. By using a crystallization plate holder replacing the mini-kappa goniostat the diffractometer can be used with CrystalDirect[TM] (Cipriani *et al.*, 2012; Marquez *et al.*, 2014) plates for *in situ* data collection. Both beamlines are equipped with PILATUS 6M-F

detectors (DECTRIS AG, Baden, Switzerland) and sample mounting robots MARVIN (in-house development EMBL Hamburg). To ensure a robust network connectivity between the beamline components a subnetwork infrastructure clearly separated from the institute's main network is deployed. Before an experiment users can submit information about their samples and experiment conditions to the ISPyB system (Delageniere *et al.*, 2011). During the experiment for rapid transfer of data collected at a beamline an InfiniBand connection between PPUs (Pilatus Processing Units) acting as a primary data storage and a secondary data storage system is used. After a user visit experimental data are kept for several weeks. Processing results and information about the experiment are available also by remote access in ISPyB. Figure 1. describes the connection between beamline components accessible by the user.
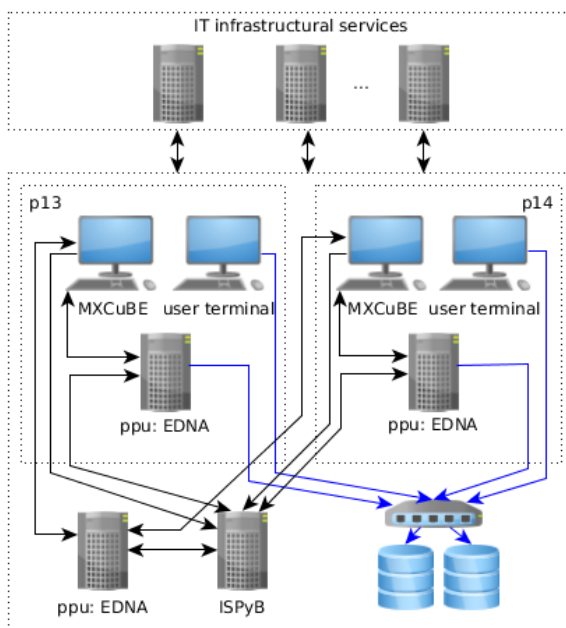

Figure 1: Beamline components and network topology for EMBL beamlines P13 and P14. At both beamlines the interaction of the user with the beamline takes place via a computer running MxCuBE. On the fly data processing is performed on a local PPU, while manual processing takes place on an additional PPU that can also serve as a hot spare in case one of the other PPUs fails. All network connections between these components are 1 Gbit/s (black arrows). High data rate InfiniBand connections connect the PPUs to the centralized TByte high performance (aggregated 1 GB/s write speed) storage (blue arrows). The ISPyB services run on a separated dedicated server. For data processing and structure solution dedicated multi-core systems with high-end graphics cards are deployed on each beamline user terminal.

For instrument control the TINE control system is used. TINE (Three-fold Integrated Networking Environment, P. Bartkiewicz, P. Duval, 2007) is a multi-platform, multi-protocol, and multi-architecture control system initially developed at DESY for the control of particle accelerators. It is based on a client-server principle with plug-and-play capabilities. For integration TINE includes client and server APIs for a wide range of programming languages and other instrument control environments (C, Java, Visual Basic, python, Labview, Matlab). All beamline devices are accessed via TINE device servers (Pazos *et al.*, 2008; Ristau *et al.*, 2014; Cianci *et al.*, 2016).

2. Experimental control and data management interfaces
To provide users with an intuitive and robust interface to complex beamline functionalities, the MxCuBE interface for experimental control is used. Initially developed and supported by the European Synchrotron Radiation Facility (ESRF) MxCuBE is widely used in synchrotrons across Europe since 2005.

2.1. Middleware TINE services
While in earlier implementations of MxCuBE high-level beamline control operations, e.g. data acquisition sequences were implemented via SPEC (Certified Scientific Software, ESRF)

commands or macros, on P13 and P14 such tasks requiring coordinated operation of more than one device are implemented into a set of middleware TINE services. For example, the TINE Energy Server simultaneously controls the undulator gap, the Bragg axis of the monochromator, and the second monochromator crystal to perform a change of X-ray energy. A TINE Transmission Server controls the configuration of attenuators for automatically setting the transmission as a function of energy. A dedicated TINE server combining both energy tuning and transmission adjustments provides an integrated functionality for the automatic acquisition of energy scans and X-ray fluorescence spectra. Crystallographic data acquisition is performed via the TINE Detector Server which coordinates the actions of the safety interlock, the Energy and Transmission Servers, the diffractometer, detector positioning, 2D X-ray detector, and a mechanical crash protection system. Further TINE services control the data management tools (in case of PILATUS detector the Furka and Grimsel tools as supplied by DECTRIS), and the rapid data delivery to the diffraction image display (ADXV, Arvai, 2015). The implementation of most middleware services follows the general architecture described in Franke *et al.* 2012.

2.2. MxCuBE implementation

MxCuBE is written in Python and accessible as an open source project through GitHub (https://github.com/mxcube/mxcube). The architecture of MxCuBE is divided in two major parts: a hardware control layer implementing the actual connections to the beamline devices and a user interface layer (Guijarro *et al.*, 2004). In the hardware control layer a hardware repository acts as a container of individually configurable hardware objects and is used as a data dispatcher. APIs to major control systems like EPICS, Tango, Sardana as well as to TINE middleware services are available. With respect to the user interface layer a Qt4-based version of MxCuBE is currently deployed at EMBL Hamburg. The Qt interface allows a fast and rapid implementation of new graphical objects and is easily adaptable to evolving MX experimental strategies. With respect to the previous version some changes were made to the overall layout to improve the ergonomics (Figure 2). The image from the MD2/3 on-axis viewing system (OAV, Cipriani F.,
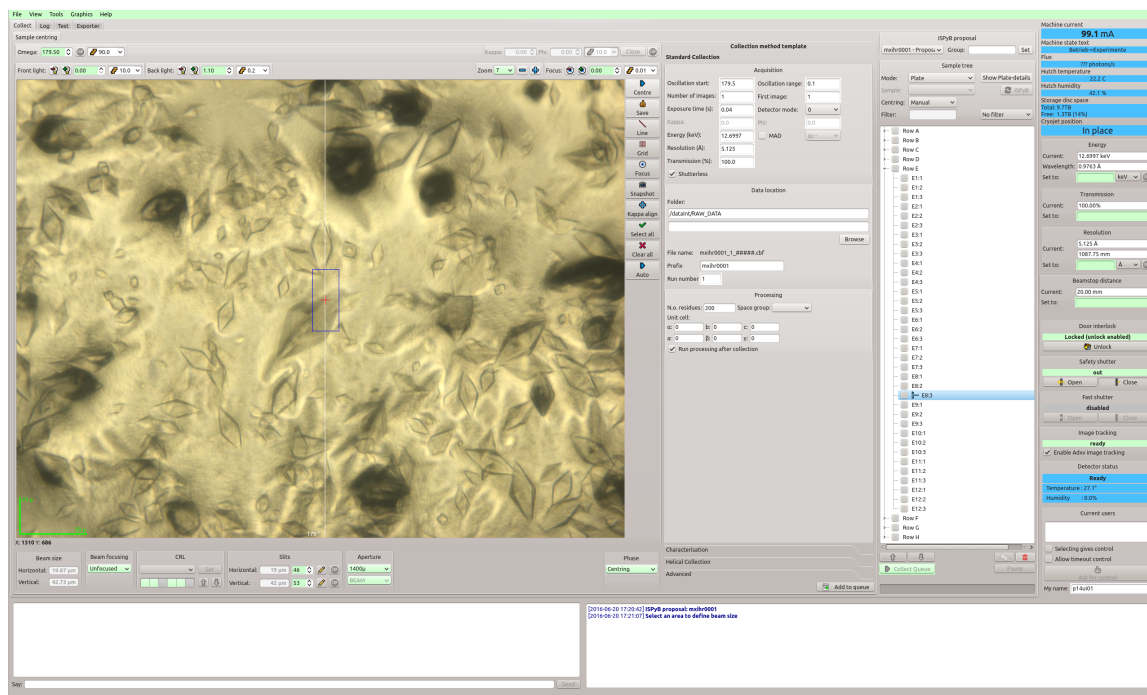

Figure 2: Graphical layout of MxCuBE Qt4 at EMBL Hamburg.

Castanga J. C., 2005) is displayed on the left-hand side of the MxCuBE main window. Tools to control sample position and orientation, change of focusing plane, lighting, zoom levels, etc. are grouped with this display. Controls for choosing different beamline optics configurations and for defining beam shapes are located underneath the OAV display. In the central part of MxCuBE the user can choose the data collection method and assign it to the respective sample. On the right-hand side status information about the beamline and synchrotron is displayed.

2.3. Serial helical line scans

Evolving macromolecular crystallographic experiments require more complex data acquisition and processing techniques, and more elaborate graphical user interfaces. At EMBL Hamburg we recently introduced the serial helical line scan data collection method (Gati *et al.*, 2014). In a serial helical line scan (SHLS) a rectangular region of interest in a sample consisting of crystals and matrix material in which the crystals are embedded is systematically exposed with an X-ray beam. Each helical scan involves a simultaneous translation and rotation of the sample with respect to the X-ray beam along a straight line (Flot *et al.*, 2010). While a crystal is traversing the X-ray beam during a helical scan a small rotation data set (Arndt U. W., 1968) is collected. By performing a series of helical scans any crystal present in the region of interest is hit by the X-ray beam and diffraction data is collected. Analysis of the images acquired in terms of whether or not diffraction patterns are detected and whether they originate from the same or from different crystals is performed subsequently. In our implementation of MxCuBE a serial helical line scan data collection starts with defining the region of interest that is mapped into the coordinate system of the diffractometer (Figure 3a and 3b). The user then chooses the data
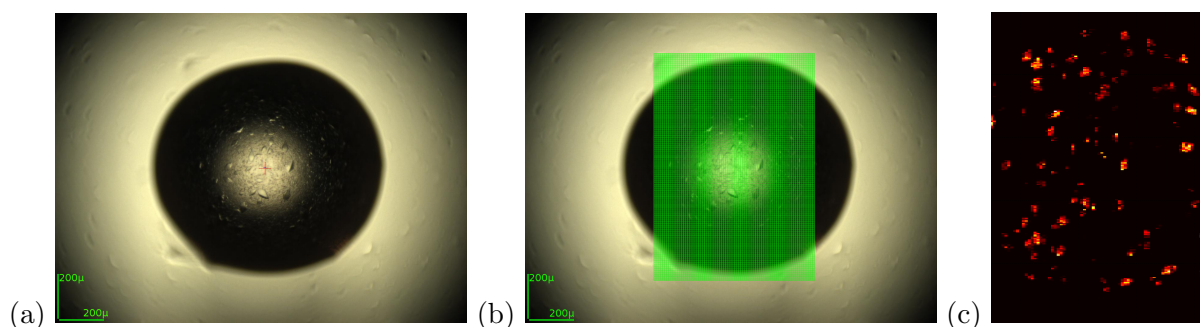

Figure 3: Serial helical line scan data collection. (a) Crystallization drop in a CrystalDirect^{TM} plate containing crystals as seen in the OAV image. (b) Definition of the region of interest to be covered by SHLSs. (c) Heatmap representing the diffraction quality observed across the region of interest defined in (b).

collection parameters including the number of parallel helical lines, the number of frames to be collected during each helical line, exposure time per frame, rotation range per helical scan, X-ray energy, and X-ray transmission. All data collection parameters are then sent to the the TINE detector server that executes the collection sequence. The general sequence involves validation of the input parameters, adjustment of the X-ray energy, transmission and resolution if requested, re-calibration of the detector if necessary, preparation of the diffractometer and the detector, for example, setting it up for multiple external triggers, opening the detector cover, starting the collection, and waiting for the detector and the diffractometer to finish. After the collection starts MxCuBE launches remote EDNA (Incardona *et al.*, 2009) parallel processing based on the DOZOR (Popov A. N., Bourenkov G. P., 2015) plugin to analyse the frames collected in terms of diffraction signals in real time. Processing results are sent back to MxCuBE via an xml-rpc server proxy. The results of the analysis are mapped onto a two-dimensional grid

implemented as a hardware object (graphics manager) for assembling a heatmap of diffraction quality. The heatmap is presented to the user in MxCuBE in real time (Figure 3c). Once an SHLS is completed the heatmap becomes interactive for controlling a number of actions:

- Selecting different properties (total DOZOR score, number of diffraction spots, resolution, etc.) as a base for the heatmap.
- Inspecting a frame related to a specific element of the heatmap by clicking on the element of the heatmap.
- Physically moving the sample to a center position corresponding to an element of the heatmap by double-clicking.
- Creating a centring point for a subsequent data collection based on the location on the heatmap.
- Filtering scan results and automatically creating centring points for further data collections (Figure 4).
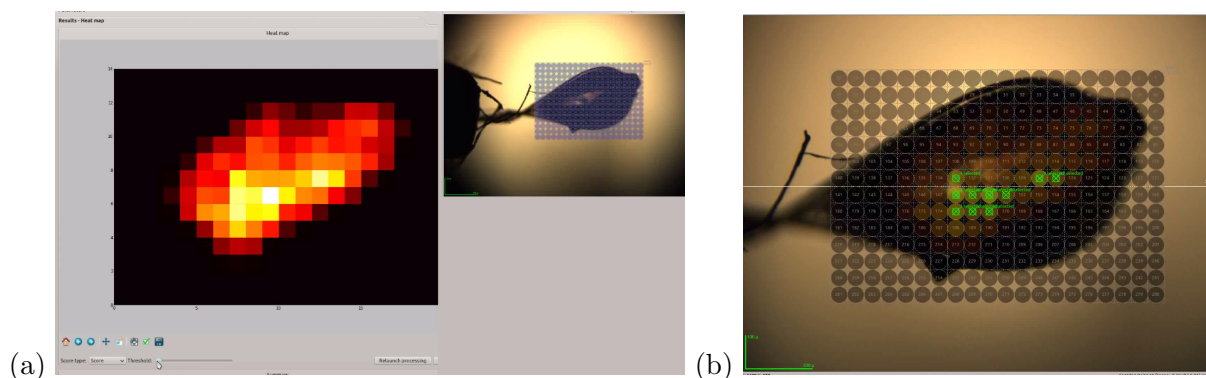

Figure 4: Heatmap-based interaction with MxCuBE. (a) Relation between heatmap and physical sample; (b) Creation of centring points based on mesh scan results.

2.4. Beam focusing tool

Apart from the data acquisition capacities MxCuBE includes various beamline alignment, customization, and testing tools. For example, at beamline P14, a widget allows switching the beam focusing between micro-focused and unfocused mode within 20 seconds (Figure 5).
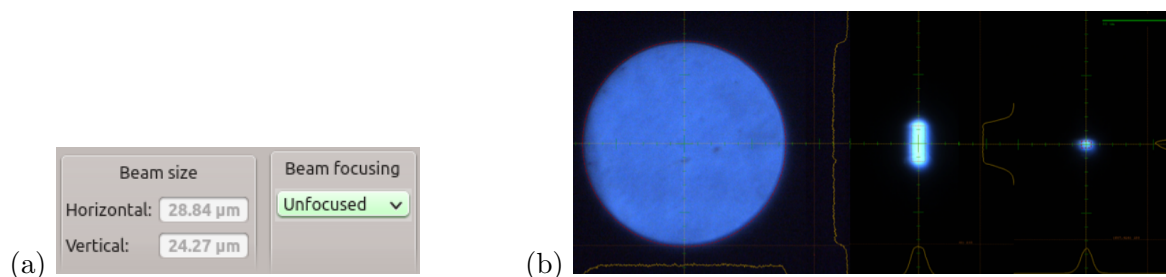

Figure 5: Beam options configuration. (a) Widget for controlling beam size and focusing configuration; (b) Unfocused, vertically and micro-focused beams as imaged on the scintillator built into the MD3 diffractometer; the diameter of the unfocused beam is approximately 150μm.

The underlying hardware object acts on a collection of 12 motors in 4 groups (detector translation, beam control unit, experimental table and KB mirrors). TINE motor servers provide data (current position, status, velocity, etc.) about each group and depending on the requested configuration MxCuBE assembles the commands for the accurate positioning of the KB-mirrors.

3. Conclusion and future perspectives

EMBL Hamburg operates two macromolecular crystallography beamlines equipped with high-end instrumentation using a combination of the TINE and MxCuBE instrument control systems. MxCuBE as an experimental control interface is well suited and capable of including new data collection methodologies. The tight and fruitful MxCuBE collaboration encourages the standartization of beamline user interface across many beamlines and provides the same look-and-feel to the users at different facilities. Future developments are geared towards (1) increasing the robustness of the system both in terms of avoiding undefined states of the beamline and in terms of not permitting operator induced errors (2) improving the ergonomy of the user interface especially in terms of implementing intuitive and precise control of complex experimental scenarios (3) making the interaction with laboratory information management system both on the sample and on the data side seamless (4) improving diagnostic tools and procedures for trouble-shooting.

4. References

[1] Arndt, U.W., Wonnacott, A.J, The Rotation Method in Crystallography, North Holland, Amsterdam (1977)

[2] Bartkiewicz P., Duval. P. *Measurement Science and Technology*, **18** (2007), p. 2379

[3] M. Cianci, M. R. Groves, D. Barford and T. R. Schneider (2015) Acta Cryst. D**72**, 403-412

[4] Cianci, M., Bourenkov, G., Karpics, I., Kallio, J., Pompidor, G., Roessle, M., Cipriani, F., Fiedler, S. & Schneider, T. R. (2016). Submitted.

[5] Cipriani, F., Felisaz, F., Lavault, B., Brockhauser, S., Ravelli, R., Launer, L., Leonard, G. & Renier, M. (2007). *AIP Conference Proceedings* **879**, 1928-1931.

[6] Cipriani F, Rower M, Landret C, Zander U, Felisaz F, et al. (2012) *Acta Cryst.* D **68**: 1393-1399

[7] Delageniere, S., Brenchereau, P., Launer, L., Ashton, A. W., Leal, R., Veyrier, S., Gabadinho, J., Gordon, E. J., Jones, S. D., Levik, K. E., McSweeney, S. M., Monaco, S., Nanao, M., Spruce, D., Svensson, O., Walsh, M. A. & Leonard, G. A. (2011). *Bioinformatics* **27**, 3186-3192.

[8] Flot, D., Mairs, T., Giraud, T., Guijarro, M., Lesourd, M., Rey, V., van Brussel, D., Morawe, C., Borel, C., Hignette, O., Chavanne, J., Nurizzo, D., McSweeney, S. & Mitchell, E. (2010). *J. Synchrotron Rad.* **17**, 107-118

[9] Franke D, Kikhney AG, Svergun DI. *Nucl Instrum Methods A.* 2012;689:5259.

[10] Gabadinho, J., Beteva, A., Guijarro, M., Rey-Bakaikoa, V., Spruce, D., Bowler, M. W., Brockhauser, S., Flot, D., Gordon, E. J., Hall, D. R., Lavault, B., McCarthy, A. A., McCarthy, J., Mitchell, E., Monaco, S., Mueller-Dieckmann, C., Nurizzo, D., Ravelli, R. B., Thibault, X., Walsh, M. A., Leonard, G. A. & McSweeney, S. M. (2010). *J Synchrotron Radiat* **17**, 700-707.

[11] Gati C, Bourenkov G, Klinge M, Rehders D, Stellato F, Oberthur D, Yefanov O, Sommer BP, Mogk S, Duszenko M, Betzel C, Schneider TR, Chapman HN, Redecke L. (2014) *IUCrJ* **1** (Pt 2):87-94

[12] Guijarro, M., Berruyer, G., Klora, J. & Rey-Bakaikoa, V. (2004). *Nobugs 2004 Conference*, Villigen PSI, Switzerland, paper 00065

[13] Incardona, M.-F., Bourenkov, G. P., Levik, K., Pieritz, R.A., Popov, N. & Svensson, O. (2009). *J. Synchrotron Rad.* 16, 872-879

[14] Marquez JA, Cipriani F. Structural Genomics, vol 1091. *Methods Mol. Biol.* **1091**:197-203

[15] Pazos, A., Ristau, U. & Fiedler, S. (2008). *PCaPAC08*, edited by PCaPAC-CERN. Ljubljana, Slovenia

[16] Popov, A. N. & Bourenkov, G. P. (2015). DOZOR. European Synchrotron Radiation Facility, Grenoble, France

[17] Ristau, U., Kolozhvari, A. & Fiedler, S. (2014). *PCaPAC2014*, edited by PcaPAC-CERN.

[18] Vaughan *et al.*, *J Synchrotron Radiat.* 2011 Mar 1; 18(Pt 2): 125-133

[19] Zander, U., Bourenkov, G., Popov, A. N., de Sanctis, D., Svensson, O., McCarthy, A. A., Round, E., Gordeliy, V., Mueller-Dieckmann, C. & Leonard, G. A. (2015). *Acta Cryst.* D**71**, 2328–2343.